ACS Catalysis

Research Article

pubs.acs.org/acscatalysis

Methanol Usage in Toluene Methylation with Medium and Large Pore Zeolites

John H. Ahn,[†] Robin Kolvenbach,[†] Sulaiman S. Al-Khattaf,[‡] Andreas Jentys,[†] and Johannes A. Lercher*[,†]

[†]Department of Chemistry, Technische Universität München, Lichtenbergstraße 4, 85747 Garching, Germany

[‡]Center of Research Excellence in Petroleum Refining and Petrochemicals, King Fahd University of Petroleum & Minerals, Dhahran 31261, Saudi Arabia

Supporting Information

ABSTRACT: The reaction of toluene methylation was investigated with four acidic zeolites of different pore geometries: the medium pore zeolites H-ZSM5 and H-ZSM11 as well as the large pore zeolites H-MOR and H-BEA. The methylation, methanol consumption, light hydrocarbon formation, and disproportionation rates for the reaction of toluene, *p*-xylene, and 1,2,4-trimethylbenezene with methanol were determined. The products of toluene methylation (e.g., xylenes and trimethylbenzenes) were readily methylated further in both medium and large pore zeolites. A considerably higher fraction of methanol was used to form light hydrocarbons with the medium pore zeolites than with large pore zeolites. This was related to the fact that the dealkylation of light hydrocarbons from highly methylated aromatics became more favorable relative to methylation at an earlier stage, that is, after fewer methyl groups were added to the aromatic ring. Increasing the effective residence time of bulky aromatic molecules with medium pore zeolites, modified either by coating the surface with tetraethyl orthosilicate or by increasing the intracrystal pore length, converted a larger fraction of methanol to light hydrocarbons via methylation and subsequent dealkylation of light hydrocarbons.

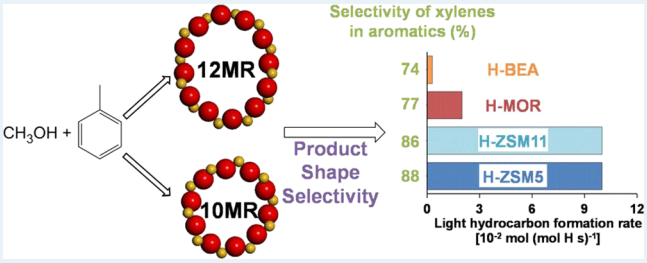

KEYWORDS: *toluene methylation, methanol to hydrocarbons, hydrocarbon pool cycle, petrochemical upgrade, acid chemistry in zeolites*

INTRODUCTION

Benzene, toluene, and xylenes are important raw materials for a variety of petrochemical commodities.[1−3] The majority of these molecules are generated via catalytic reforming or as byproducts of naphtha cracking.[2,3] Among the three, toluene is produced in excess relative to the market demand[1] and methylation of toluene to xylenes would, therefore, be a potential way to balance the deficiency of xylene production.

In toluene methylation, methanol (MeOH) reacts with a toluene to form a xylene (Scheme 1). Under typical reaction conditions, this reaction is accompanied by several side reactions leading to light hydrocarbons (LH)[4−7] and further methylated aromatics, for example, trimethylbenzene (TriMB) and tetramethylbenzene (TetraMB).[5,8−10] Many research groups have thus used an excess of toluene relative to methanol[6,11−13] to avoid formation of these side products, albeit with the drawback of lower maximum toluene conversions and relatively high selectivity to light hydrocarbons. Inefficient methanol usage, even in an excess of toluene relative to methanol, is thus one of the major drawbacks for the process commercialization[3] and has not been resolved.

Thus, we selected four different acidic zeolites to gain insight into the use of methanol during toluene methylation: H-ZSM5, H-ZSM11, H-MOR and H-BEA. The first two are medium-pore-sized zeolites (10-membered ring (MR)), and the latter two are large-pore-sized zeolites (12-MR). The data here indicated that most of the methanol was used for methylation of toluene and its aromatic products (e.g., xylenes and TriMBs), but the dealkylation of light hydrocarbons from highly

Scheme 1. The Reaction of Toluene Methylation with Methanol[a]

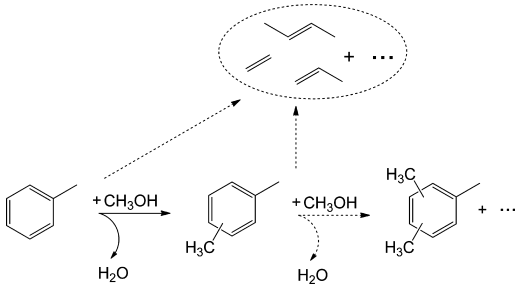

[a]The formation of undesired side products during the reaction, such as light hydrocarbons and trimethylbenzenes, are indicated by dashed arrows.

Received: January 30, 2013
Revised: March 11, 2013
Published: March 12, 2013

methylated aromatic molecules eventually became more favorable relative to methylation because of product shape selectivity.[14] The multiple aromatic methylation and the subsequent dealkylation is a well-discussed reaction pathway for the formation of light hydrocarbons during methanol-to-hydrocarbon reactions.[9,15−17] The formation of ethene as well as some propene[18] is likely to occur by side-chain methylation (via methylation of the methyl group of an aromatic ring) or by a paring mechanism (via aromatic ring contraction and expansion).[19,20] In this work, we provide clear evidence that such a reaction route also plays an important role in the use of methanol during the toluene methylation reaction.

EXPERIMENTAL SECTION

Materials. The materials H-ZSM5 (Si/Al = 36), H-MOR (Si/Al = 45), and H-BEA (Si/Al = 75) were provided by Süd-Chemie, and H-ZSM11 was synthesized by using tetrabutylammonium hydroxide (TBAOH; ≥99.0%, 30-hydrate, Sigma Aldrich) and 1,8-diamino-octane (DAO; 98%, Sigma Aldrich) as the organic templates for small- (SC) and large-crystal (LC) zeolites, respectively.[21,22] Aluminum nitrate (≥98%, non-ahydrate), fumed silica (Cab-O-sil M-5), and sodium hydroxide (≥98%) were used for SC H-ZSM11 synthesis, and aluminum sulfate (99.99%), potassium hydroxide (99.99%), and silica sol (Ludox AS-30) were used for LC H-ZSM11 synthesis (all purchased from Sigma Aldrich). The gel composition for SC H-ZSM11 was $9TBAOH/Al_2O_3/90SiO_2/1065H_2O/6.5Na_2O$. The uniform mixture was aged overnight and transferred into Teflon liners and sealed inside autoclaves. The crystallization time was 18 h at 448 K under rotation (60 rpm). The gel composition for LC H-ZSM11 was $26DAO/Al_2O_3/90SiO_2/3580H_2O/12K_2O$. This mixture was aged for ∼1 h before it was transferred into Teflon liners and sealed inside autoclaves. The crystallization time was 72 h at 433 K under static conditions.

After the desired crystallization time, the autoclaves were cooled under water, and the solids were separated by centrifugation and washed three times with deionized water. The samples were dried in an oven at 353 K, ground, and treated at 823 K (heating rate of 0.05 K s^{-1}) for 10 h in synthetic air (flowing at 1.67 cm^3 s^{-1}; 20.5% O_2 in N_2, Westfalen) to remove the organic templates.

After the template removal, ammonium ion exchange was carried out at 353 K under stirring for 6 h in a 0.2 M NH_4Cl solution (30 cm^3 per gram of zeolite). This procedure was repeated three times. After the third ammonium exchange, the zeolites were separated by centrifugation, washed, dried, and treated in synthetic air (flowing at 1.67 cm^3 s^{-1}) for 10 h (heating rate of 0.05 K s^{-1}) at 823 K to obtain the protonic form of the zeolite.

The surface-modified (SM) sample of H-ZSM5 was prepared by heating 10 g of zeolite in 250 cm^3 of hexane (>97%, Sigma Aldrich) containing 1.5 cm^3 of tetraethyl orthosilicate (TEOS; 4 wt % SiO_2 relative to the zeolite; >99.0%, Sigma Aldrich) at 353 K under stirring for 1 h.[23] Hexane was removed by a rotary evaporator under vacuum, and the sample was dried at 353 K and subsequently treated in a synthetic air (flowing at 1.67 cm^3 s^{-1}) at 353 K (0.083 K s^{-1}) for 2 h; at 453 K (0.033 K s^{-1}) for 3 h; and finally, at 823 K (0.033 K s^{-1}) for 5 h. This procedure was repeated three times before the material was characterized and tested (total deposition amount of 12 wt % SiO_2).

Catalyst Characterization. The elemental composition of the zeolites was determined by atomic absorption spectroscopy (AAS; Unicam M Series Flame-AAS equipped with an FS 95 autosampler and a GF 95 graphite furnace), and the purity and crystallinity of the samples were examined by X-ray diffraction (XRD; Philips X'Pert Pro system, $\lambda_{Cu\ K\alpha}$ = 0.154 056 nm, 40 kV/40 mA) recorded between 2θ angles of 5−70° (step size of 0.017° and a scan speed of 115 s/step). Nitrogen physisorption measurements were carried out at 77 K on a PMI automated sorptometer after outgassing the samples under vacuum at 523 K for 2 h. The BET surface area[24] was calculated from the nitrogen adsorption data over a relative pressure range from 0.01 to 0.1 p/p_0. The pore volumes and external surface areas were evaluated by using the *t*-plot method[25] according to Halsey.[26] The scanning electron microscopy (SEM) images of all samples were recorded on a JEOL JSM 5900LV microscope operating at 25 kV. The characteristic diffusion times of medium pore zeolites were determined by measuring *o*-xylene uptake rates by flowing 2.1 cm^3 s^{-1} of helium to a self-supporting wafer in a cell (1.5 cm^3), using infrared spectroscopy (Thermo Nicolet 6700 FT-IR spectrometer, resolution of 4 cm^{-1}). The sample was activated at 523 K (heating rate of 0.17 K s^{-1}) under flowing helium for 12 h before switching to a second helium stream (2.1 cm^3 s^{-1}) with saturated *o*-xylene (0.05 kPa). The spectra were measured every 60s at 403 K and were normalized to the integral of the overtone lattice band between 2105 and 1740 cm^{-1} of the activated H-ZSM5 sample. The characteristic ring vibrations of *o*-xylene at 1496 and 1466 cm^{-1}[27] were integrated and normalized to the steady state integral to determine the characteristic diffusion time (L^2/D_{app}) with the equation below:

$$\frac{m}{m_\infty} = 1 - \sum_{n=1}^{\infty} \frac{6}{n^2\pi^2} \exp\left(\frac{-n^2\pi^2 D_{app} t}{L^2}\right) \quad (1)$$

Here, m and m_∞ are the uptake at time t and after equilibration, respectively, D_{app} is the apparent diffusion coefficient, and L is the average crystal size of a zeolite.

Infrared spectroscopy (Thermo Nicolet 5700 FT-IR spectrometer, resolution of 4 cm^{-1}) with pyridine (99.8%, Sigma Aldrich) as probe molecule was used to determine the total concentration of Brønsted and Lewis acid sites. The spectrum of an activated sample (pressed into a self-supporting wafer with density of ∼0.01 g cm^{-2}) was measured at 423 K after evacuating for 1 h at 723 K (heating rate of 0.17 K s^{-1}). Pyridine was adsorbed on the zeolite at 0.01 kPa, 423 K for 0.5 h and outgassed for 1 h under vacuum to desorb weakly bound species. The total concentration of Brønsted and Lewis acid sites was determined by integrating the peaks at 1546 and 1455 cm^{-1}, respectively.

Catalytic Testing. The catalysts (180−250 μm particle size) and silicon carbide (7 times the weight of the catalyst; F46, ESK-SiC GmbH), held in place by quartz wool inside a quartz plug flow reactor (0.4 cm ID), were activated at 823 K (heating rate of 0.17 K s^{-1}) under flowing He (1.7 cm^3 s^{-1}; 99.996%, Westfalen) prior to the reaction. The temperature was measured by a thermocouple in external contact with the reactor and was maintained constant by a stainless steel furnace connected to a Eurotherm controller (series 2416). The catalysts were tested at 673 K at 101 kPa by flowing a premixed feed of toluene (>99.9%, Sigma Aldrich) or *p*-xylene (>99%, Sigma Aldrich) or 1,2,4-trimethylbenzene (98%, Sigma Aldrich) with methanol (>99.8%, Sigma Aldrich) into a vaporizer filled with silicon carbide. The total flow rate was 2.3 cm^3 s^{-1}, and the aromatic to methanol molar ratio was 4, with $p_{aromatic}$ = 1.2−6 kPa and $p_{methanol}$ = 0.3−1.5 kPa. The reactor effluent was

dx.doi.org/10.1021/cs4000766 | ACS Catal. 2013, 3, 817−825

Table 1. The Channel Size and Dimensions, Chemical Compositions, Textural Properties and Acid Site Concentrations of All Zeolite Samples Tested

	catalyst					
	H-ZSM5	H-ZSM11-SC[a]	H-MOR	H-BEA	H-ZSM5-SM[b]	H-ZSM11-LC[c]
channel size and connectivity (10^{-1} nm)	{5.1 × 5.5 5.3 × 5.6}***	5.3 × 5.4***	{6.5 × 7 2.6 × 5.7}***	6.6 × 6.7** 5.6 × 5.6*	{5.1 × 5.5 5.3 × 5.6}***	5.3 × 5.4***
Si/Al ratio[d]	36 (36)	34 (33)	43 (40)	79 (82)	42 (39)	33 (30)
S_{BET}[e] (m^2 g^{-1})	435	445	584	718	434	427
S_{ext}[f] (m^2 g^{-1})	55	110	81	189	74	2
V_{mi}[g] (cm^3 g^{-1})	0.16	0.13	0.18	0.20	0.13	0.16
Brønsted acid (μmol g^{-1})	380	387	307	175	336	424
Lewis acid (μmol g^{-1})	67	100	98	24	73	112

[a]SC = small crystal. [b]SM = surface modified sample with TEOS. [c]LC = large crystal. [d]Si/Al ratio calculated from the acid concentration from the pyridine adsorption is shown in parentheses. [e]S_{BET} = BET surface area. [f]S_{ext} = external surface area, calculated from *t*-plot method (Halsey). [g]V_{mi} = micropore volume, calculated from *t*-plot method (Halsey).

sampled ~0.75 h after the start of the reactant flow into the reactor and was analyzed by online gas chromatography (Agilent 7820A) using a DB-WAX column (30 m × 0.32 mm × 0.5 μm) and a flame ionization detector. The product selectivities did not change significantly with the reaction time (the time-on-stream behavior of medium (H-ZSM5) and large (H-BEA) pore zeolites are summarized in Table S1 of the Supporting Information).

The rates of methylation (toluene, *p*-xylene, and 1,2,4-TriMB; based on consumption) were calculated by multiplying the aromatic feed rate per gram of zeolite in the reactor (mol g^{-1} s^{-1}) by the conversion of the reactant aromatic molecule (%; the isomers, e.g., *o*- and *m*-xylene when *p*-xylene was co-fed with methanol, were treated as reactants) and dividing it by the concentration of Brønsted acid sites (mol H^+ g^{-1}), determined by the adsorption of pyridine. The formation rates of light hydrocarbon were calculated by multiplying the rate of total carbons in the feed per gram of zeolite in the reactor by the carbon selectivity of light hydrocarbons formed and dividing it by the concentration of Brønsted acid sites.

RESULTS

Catalyst Characterization. The micropore structure and dimensions, the chemical compositions, textural properties, and acid site concentration of all zeolite samples derived from atomic absorption spectroscopy, nitrogen physisorption, and IR spectra of adsorbed pyridine are summarized in Table 1. The total concentration of acid sites (Brønsted and Lewis) determined by adsorption of pyridine agreed well with the values calculated from the Si/Al ratios (within ±10%). The Brønsted acid site concentration of H-BEA sample was lower than the others used here, but the lower acid site concentration of H-BEA did not significantly affect the fraction of methanol usage calculated (section 3.3; see also Supporting Information Tables S2–S3).

The XRD of synthesized H-ZSM11 (small and large crystals) indicated that both materials are free of crystalline impurities (Supporting Information Figures S1 and S2). Narrower XRD peaks of large crystal sample suggest that the primary crystal size is significantly larger than that of small crystal H-ZSM11. The SEM images of all samples are shown in the Supporting Information (Figures S3–S8). The particle for all samples was around 0.5 μm or less, except for the large crystal H-ZSM11 sample (~6 μm).

Methylation of Toluene in Medium and Large Pore Zeolites. The reactant (C_1 and toluene) conversions, selectivity of xylenes in aromatics, toluene methylation, and light hydrocarbon formation rates on both medium and large pore zeolites are shown in Table 2. Here, the C_1 refers to methanol and dimethyl ether (DME), and we treat them as one reactant (accounting for the fact that DME has twice as many carbon atoms as MeOH) because methanol can reversibly dehydrate to DME under typical reaction conditions, and DME can be used to methylate unsaturated aromatic/alkene molecules via similar mechanisms.[28,29] The reaction order of toluene methylation was between zero and first with respect to methanol and first with respect to toluene under the reaction conditions used (see Supporting Information Figures S9–10). Small crystal H-ZSM11 was used for all catalytic tests unless indicated otherwise, and the catalyst amount was adjusted to keep the C_1 conversion (the limiting reactant) at a comparable range. The rate of toluene methylation was similar for all zeolites, but the xylene selectivity was somewhat higher and the light hydrocarbon formation rates significantly higher for the medium compared with the large pore zeolites.

Table 2. C_1 and Toluene Conversion, Xylene Selectivity, Toluene Methylation and Light Hydrocarbon Formation Rates[a] with Medium[b] and Large[c] Pore Zeolites in Toluene Methylation

	catalyst			
	H-ZSM5	H-ZSM11	H-MOR	H-BEA
C_1 conversion[d] (%)	55	64	55	53
toluene conversion (%)	6.4	7.9	9.4	8.7
xylenes in aromatics (%)	88	86	77	74
toluene methylation rates[e] [10^{-2} mol (mol H $s)^{-1}$]	16	17	15	15
light hydrocarbon formation rates [10^{-2} mol C (mol H $s)^{-1}$]	10	10	2.0	0.3

[a]Reaction rates are measured at $p_{toluene}$ = 6 kPa, $p_{methanol}$ = 1.5 kPa, 673 K, 6–20 mg of catalyst, and 2.3 cm^3 s^{-1} total flow rate. [b]H-ZSM5 and H-ZSM11. [c]H-MOR and H-BEA. [d]C_1 is methanol and DME (both are treated as the same reactant because methanol can be transformed into DME during the reaction and DME can also be used for methylation). [e]Calculated on the basis of toluene consumption.

Methanol Usage in Methylation of Toluene. To better define methanol usage during the methylation of toluene, three different fractional uses of reactant (based on C_1 usage) were calculated: (1) MeOH for toluene alkylation, (2) MeOH for

dx.doi.org/10.1021/cs4000766 | ACS Catal. 2013, 3, 817–825

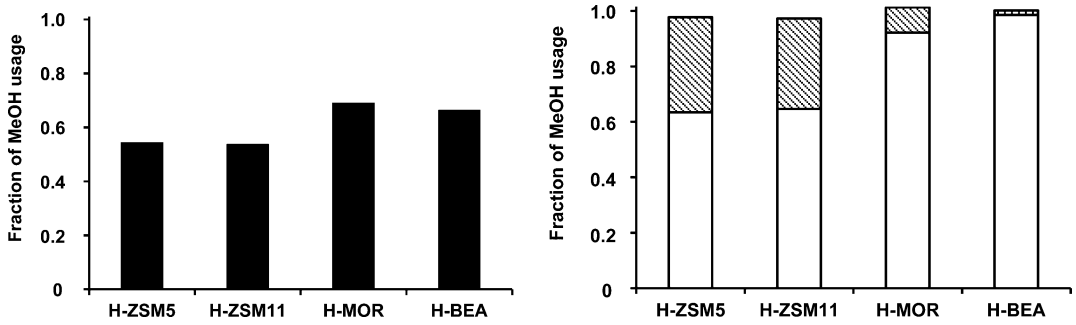

Figure 1. Fraction of MeOH used for the methylation of toluene ("MeOH for toluene alkylation"; left, solid), methylation of aromatics ("MeOH for aromatics alkylation"; right, open), and formation of light hydrocarbons ("MeOH for LH formation"; right, striped) calculated for both medium (H-ZSM5 and H-ZSM11) and large pore zeolites (H-MOR and H-BEA) at $p_{toluene}$ = 6 kPa, $p_{methanol}$ = 1.5 kPa, 673 K, 6−20 mg of catalyst, 2.3 $cm^3\ s^{-1}$ total flow rate, and C_1 conversion = 53−64%.

aromatics alkylation, (3) MeOH for LH formation. The definitions are shown below:

$$\text{fraction of Me OH for toluene alkylation} = \frac{\text{toluene}_{in} - \text{toluene}_{out} - 2 \times \text{benzene}}{\text{methanol}_{in} - (\text{methanol} + 2 \times \text{DME})_{out}} \quad (2)$$

$$\text{fraction of MeOH for aromatics alkylation} = \frac{1 \times \text{xylenes} + 2 \times \text{TriMB} + 3 \times \text{TetraMB} + \ldots}{\text{methanol}_{in} - (\text{methanol} + 2 \times \text{DME})_{out}} \quad (3)$$

$$\text{fraction of MeOH for LH formation} = \frac{2 \times C_2 + 3 \times C_3 + 4 \times C_4 + \ldots}{\text{methanol}_{in} - (\text{methanol} + 2 \times \text{DME})_{out}} \quad (4)$$

The subscripts "in" and "out" indicate the rate of reactant (toluene or methanol/DME) going in and out of the reactor, respectively. Each term in the numerator of eqs 3−4, as well as "benzene" in eq 2, is the formation rate measured (mol [s mol H]$^{-1}$). Equation 2 ("MeOH for toluene alkylation") describes the fraction of methanol (and DME) that is used for the methylation of toluene. If the fraction is equal to 1, all of methanol is used for the methylation of toluene, and this would be the ideal case. Equation 3 ("MeOH for aromatics alkylation") describes the fraction of methanol used for alkylating the aromatic ring of toluene. If the fraction is equal to 1, methanol selectively reacts with aromatic molecules and does not form light hydrocarbons. In the numerator, the moles of xylenes formed is multiplied by 1 because 1 mol of C_1 is added to the starting aromatic molecule (toluene), the moles of TriMBs formed is multiplied by 2 because 2 mol of C_1 is added to toluene. Equation 4 ("MeOH for LH formation") describes the fraction of methanol used for the formation of light hydrocarbons. If the fraction is 1, methanol forms only light hydrocarbons and is not used for the methylation of aromatics. In the numerator, the moles of C_2 (ethene and ethane) formed is multiplied, for example, by 2, because 2 mol of C_1 is used to generate C_2 species.

The methanol usage in medium pore (H-ZSM5 and H-ZSM11) and large pore (H-MOR and H-BEA) zeolites is summarized in Figure 1. With H-MOR and H-BEA (large pore zeolites), the fraction of "MeOH for toluene alkylation" was only ∼0.65−0.7 (Figure 1, left) but the fraction of "MeOH for aromatics alkylation" was very high (>0.9; Figure 1, right), and the "MeOH for LH formation", low (<0.1; Figure 1, right). A high fraction of "MeOH for aromatics alkylation" indicates that most of the methanol was utilized to methylate toluene, and the products of toluene methylation (e.g., xylenes and TriMBs), in large pore zeolites. The fraction of "MeOH for toluene alkylation" was somewhat lower (∼0.55; Figure 1, left) with H-ZSM5 and H-ZSM11 (medium pore zeolites), and unlike the large pore zeolites, the fraction of "MeOH for aromatics alkylation" was only slightly higher than the fraction of "MeOH for toluene alkylation" (∼0.65; Figure 1, right), with a relatively high fraction of "MeOH for LH formation" (∼0.35; Figure 1, right). This indicates that a considerable amount of methanol was used for the formation of light hydrocarbons in the medium pore zeolites.

Reaction of Toluene, *p*-Xylene and 1,2,4-Trimethylbenzene with Methanol. The rate of methylation (measured at the same partial pressures and similar C_1 conversion levels) of toluene, *p*-xylene, and 1,2,4-TriMB with large pore zeolites increased as the number of methyl substitutions in the aromatic ring increased. This trend was especially pronounced with H-BEA (Figure 2). An opposite trend was observed with medium pore zeolites (H-ZSM5 and H-ZSM11). The rates of light hydrocarbon formation, as well as the methanol usage toward light hydrocarbons (fraction of "MeOH for LH formation"), in large pore zeolites increased systematically with the number of methyl substitutions (Figures 3 and 4). The same trends were observed with medium pore zeolites, except that the light hydrocarbon formation rate decreased when the number of

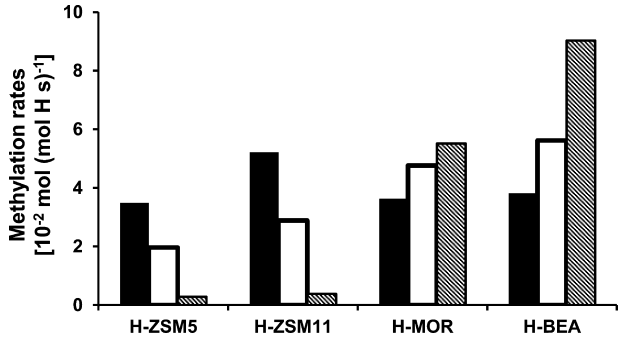

Figure 2. Rate of methylation when toluene (solid), *p*-xylene (open), or 1,2,4-trimethylbenzene (striped) reacted with methanol in both medium (H-ZSM5 and H-ZSM11) and large pore zeolites (H-MOR and H-BEA) at $p_{aromatic}$ = 1.2 kPa, $p_{methanol}$ = 0.3 kPa, 673 K, 5−12 mg of catalyst, 2.3 $cm^3\ s^{-1}$ total flow rate, and C_1 conversion = 51−58% (H-ZSM5 and H-ZSM11) and 45−50% (H-MOR and H-BEA).

dx.doi.org/10.1021/cs4000766 | ACS Catal. 2013, 3, 817−825

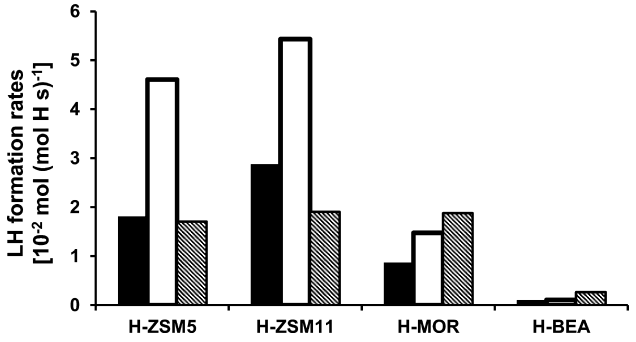

Figure 3. Rate of light hydrocarbon (LH) formation when toluene (solid), *p*-xylene (empty), or 1,2,4-trimethylbenzene (striped) reacted with methanol in both medium (H-ZSM5 and H-ZSM11) and large pore zeolites (H-MOR and H-BEA) at $p_{aromatic}$ = 1.2 kPa, $p_{methanol}$ = 0.3 kPa, 673 K, 5−12 mg of catalyst, 2.3 cm^3 s^{-1} total flow rate, and C_1 conversion = 51−58% (H-ZSM5 and H-ZSM11) and 45−50% (H-MOR and H-BEA).

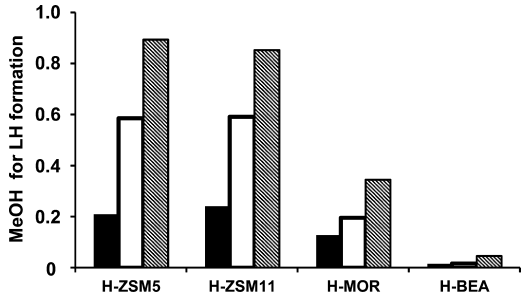

Figure 4. Fraction of methanol used for the formation of light hydrocarbons ("MeOH for LH formation") when toluene (solid), *p*-xylene (open), or 1,2,4-trimethylbenzene (striped) reacted with methanol in both medium (H-ZSM5 and H-ZSM11) and large pore zeolites (H-MOR and H-BEA) at $p_{aromatic}$ = 1.2 kPa, $p_{methanol}$ = 0.3 kPa, 673 K, 5−12 mg of catalyst, 2.3 cm^3 s^{-1} total flow rate, and C_1 conversion = 51−58% (H-ZSM5 and H-ZSM11) and 45−50% (H-MOR and H-BEA).

methyl groups increased from *p*-xylene to 1,2,4-TriMB (Figure 3).

Effect of Residence Time on Methanol Usage in Toluene Methylation. Two additional medium pore zeolites were used to investigate the relationship between the residence time of bulky methylated aromatics and the methanol usage in toluene methylation. One was prepared by coating the outer surface of H-ZSM5 with tetraethyl orthosilicate. This method partially blocked access to the pore system and increased the overall tortuosity,[11,30,31] thereby increasing the effective residence time of bulky aromatics molecules, such as *o*- and *m*-xylenes.[31] The second sample was a large crystal H-ZSM11 zeolite (SEM image is shown in Supporting Information Figure S7), for which the longer channel length should increase the effective residence time of molecules inside the micropores. For both modified samples, a higher fraction of methanol was converted into light hydrocarbons, and less was utilized for the methylation of aromatic molecules (Figure 5).

DISCUSSION

Methanol Usage in Toluene Methylation with Large Pore Zeolites. In the reaction of toluene methylation, 1 mol of toluene and 1 mol of methanol (or 0.5 mol of DME) are required to form 1 mol of xylene (Scheme 1). The methanol

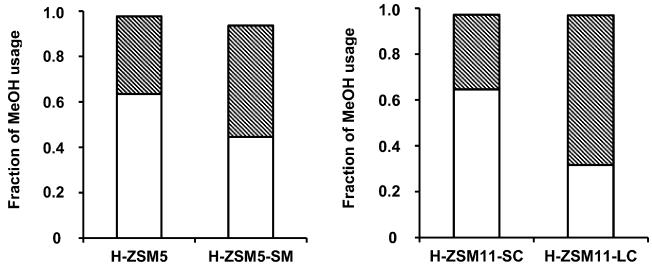

Figure 5. Fraction of methanol used for methylation of aromatics ("MeOH for aromatics alkylation" (open)) and for formation of light hydrocarbons ("MeOH for LH formation" (striped)) for H-ZSM5 (left, parent and surface-modified (SM) with TEOS) and H-ZSM11 (right, small (SC) and large crystal (LC)) at $p_{toluene}$ = 6 kPa, $p_{methanol}$ = 1.5 kPa, 673 K, 5−10 mg of catalyst, 1.7−2.3 cm^3 s^{-1} total flow rate, and C_1 conversion = 53−63%.

usage toward methylating toluene in H-MOR and H-BEA (large pore zeolites) is, however, only ∼0.65, that is, the "MeOH for toluene alkylation" fraction (Figure 1, left), despite the fact that toluene is present in 4-fold (molar) excess relative to methanol. Methanol that is not used for the methylation of toluene reacts mostly in methylating the primary aromatic products from toluene methylation, for example, xylenes and TriMBs, indicated by a high "MeOH for aromatics alkylation" fraction (Figure 1, right). About 2 mol % with respect to the total concentration in aromatics was observed as hexamethylbenzene over both large pore zeolites.

More than 20% of the C_1 converted in large pore zeolites is used for methylation of aromatics heavier than toluene, that is, xylenes to TriMBs and TriMBs to TetraMBs, even though the toluene concentration is >90% of the aromatics in the gas phase. One of the reasons for the secondary methylation is related to the fact that the activation energy for methylation decreases with increasing methyl substitution of the aromatic ring in the absence of steric hindrances.[32,33] The methyl groups are electron-donating, and increasing the number of methyl groups increases in the base strength of aromatic molecules. The rate of methylation, indeed, increases as the number of methyl substitution increases from toluene to *p*-xylene to 1,2,4-TriMB (Figure 2), and this most likely contributes to further methylation of methylated products from toluene as well as lower xylene selectivity within aromatics (relative to medium pore zeolites; Table 2).

Methanol Usage in Toluene Methylation with Medium Pore Zeolites. The methanol usage toward toluene methylation is less efficient (∼0.55; "MeOH for toluene alkylation" fraction in Figure 1, left) with H-ZSM5 and H-ZSM11 (medium pore zeolites) compared with the large pore zeolites, and a substantial fraction of methanol is converted into the light hydrocarbons (Figure 1 right). This is unexpected at first, especially because toluene is fed in a 4-fold (molar) excess compared with methanol. Thus, the formation of light hydrocarbons from methanol[34,35] is expected to play a minor role relative to the toluene methylation. Only a slight increase in "MeOH for aromatics alkylation" from "MeOH for toluene alkylation" fractions are observed (∼0.65 from 0.55, see Figure 1), indicating that the bulky xylenes and TriMB is not methylated further or able to exit the micropores very slowly due to the relatively large size of these molecules. Note that only a very small amount of TetraMB (<2 mol %) and no penta- or hexamethylbenzenes were detected in the gas phase.

dx.doi.org/10.1021/cs4000766 | ACS Catal. 2013, 3, 817−825

The kinetic results for H-ZSM5 and H-ZSM11 (Figure 2) show that the methylation rates of aromatics decrease as the number of methyl substitutions increases, which is in contrast to the theoretical simulations reported in ref 16. The calculations using a 46 T-atom ZSM5 cluster, which accounts for the steric hindrances, indicates that the reaction rate constants for methylation increase from toluene to *p*-xylene and 1,2,4-TriMB by an order of magnitude at 673 K (the activation energy of methylation also decreased).[16] Furthermore, the intersection diameter of H-ZSM5 (~0.9 nm) is larger than the kinetic diameter of the bulkiest TetraMB (0.86 nm for 1,2,3,5-TetraMB[36]). Thus, the methylation rate of aromatics in the medium pore zeolites probably does not decrease due to steric hindrances, at least for the methylation reaction occurring on Brønsted acid sites located at the intersections with the aromatic molecules tested here (1,2,4-TriMB methylates to TetraMB). The highly methylated aromatic molecules most likely methylate further, but leave the zeolite pores as less-methylated aromatics, for example, as xylenes and TriMBs, by splitting off light hydrocarbons (vide infra).

The fraction of methanol used for the formation of light hydrocarbons increases as the number of methyl groups increases in the aromatic ring (Figure 4). It is unlikely that the majority of the light hydrocarbons is generated from the direct coupling of methanol or DME because of high activation barriers[37,38] or from the alkene methylation−cracking cycle[39,40] because the aromatics concentration is much higher compared with that of alkenes under the reaction conditions used (>50:1 in the gas phase). Therefore, we expect that most of the light hydrocarbons are formed by the methylation of aromatics, followed by ring contraction−expansion (paring mechanism) or by side chain methylation with subsequent cracking.[19,20]

It is difficult to unequivocally conclude, however, that all of the light hydrocarbons are generated via this route because alkene methylation has a slightly lower energy of activation relative to the aromatic methylation.[29,41] Moreover, 1,2,4-TriMB diffuses more slowly than *p*-xylene to active sites in the micropores,[31] and consequently, the local concentration ratio of alkenes to aromatics inside the micropores with 1,2,4-TriMB as an aromatic feed relative to *p*-xylene or toluene may be higher during the reaction. Thus, the alkene methylation-cracking cycle could play a more significant role in the formation of light hydrocarbons and increase the "MeOH for LH formation" fraction (Figure 4) when 1,2,4-TriMB reacts with methanol, as compared with the reaction with *p*-xylene. The diffusivities of toluene and *p*-xylene, however, are similar,[42,43] but a significant increase in the fraction of "MeOH for LH formation" is observed from toluene to *p*-xylene as the reactant in the feed (Figure 4). The steady increase in methanol usage toward formation of light hydrocarbons with increasing methyl substitution and the similar diffusivities of toluene and *p*-xylene, therefore, indicate that most light hydrocarbons are generated from the highly methylated aromatics.

Figure 3 shows that the formation rate of light hydrocarbons increases significantly when *p*-xylene (instead of toluene) is co-fed with methanol, suggesting that the overall generation of the light hydrocarbons is limited by the rate of sequential methylation of aromatics. The computational results also show that the light hydrocarbon dealkylation step is faster than the methylation step in MFI (H-ZSM5) framework by at least an order of magnitude.[16] When 1,2,4-TriMB is used as an aromatic in the feed instead of *p*-xylene, the light hydrocarbon formation rate decreases (Figure 3), most likely because the rate coefficient of 1,2,4-TriMB methylation decreases slightly relative to *p*-xylene methylation.[16] The intraparticle diffusion of the bulkier TriMB to the active sites is also much slower than for *p*-xylene, and less aromatic molecules are, thus, available for methylation and subsequent dealkylation of light hydrocarbons.[31] Nevertheless, methanol is used more effectively for the formation of light hydrocarbons when reacting with 1,2,4-TriMB (higher methylated aromatics), as compared with the less-methylated molecules, such as *p*-xylene and toluene (Figure 4), because TriMB is closer to the point at which dealkylation is favored over methylation.

The methylation of the xylenes to TriMBs and TetraMBs continues in the zeolite pores, but it cannot be stated at which point the dealkylation to light hydrocarbons becomes more favorable, that is, how many times toluene methylates, before the rate of dealkylation becomes faster than that of methylation. We speculate that 1,2,3,5-TetraMB can be formed in medium pore zeolites and methylated further at the geminal carbon position to 1,1,2,4,6-pentamethylbenzene because the corresponding pentamethylbenzenium cation (Figure 6) has been

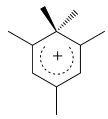

Figure 6. 1,1,2,4,6-Pentamethylbenzenium cation.

observed by NMR spectroscopy (formed most likely in the channel intersections) when toluene reacts with methanol.[44] Note that it is possible for penta- and hexamethylbenezene also to form inside the zeolite pores, but these species were only indirectly detected, that is, by dissolving the used zeolite in HF.[45]

The dealkylation reactions from highly methylated aromatic molecules increase the selectivity of light hydrocarbon molecules (undesired byproducts) in toluene methylation. The comparison of disproportionation and methylation rates for toluene, *p*-xylene or 1,2,4-TriMB when co-fed with methanol, is shown in Table 3. The disproportionation rates are calculated as the equations shown below:

$$\text{disproportionation rate of toluene} = 2 \times \text{formation rate of benzene} \quad (5)$$

$$\text{disproportionation rate of } p\text{-xylene} = 2 \times \text{formation rate of toluene} \quad (6)$$

$$\text{disproportionation rate of 1,2,4-TriMB} = 2 \times \text{formation rate of all xylenes} \quad (7)$$

The contribution to the products from disproportionation (e.g., benzene from toluene) increases as the number of methyl groups in the aromatic ring increases (% reacted aromatic consumed for disproportionation in Table 3). These products result either from the disproportionation or demethylation or from a reaction involving the cleavage of a light hydrocarbon from a highly methylated aromatic molecule.

Only a minor quantity of disproportionation products (i.e., benzene and toluene) relative to methylation products are observed when toluene or *p*-xylene reacts with methanol, but the contribution of the disproportionation increases significantly for the reaction with 1,2,4-TriMB, as indicated by a large

dx.doi.org/10.1021/cs4000766 | ACS Catal. 2013, 3, 817−825

Table 3. C_1 Conversion, Methylation and Disproportionation Rates[a], Percent of Reacted Aromatic Molecule Consumed for Disproportionation, And Xylene Isomer Selectivity with H-ZSM5 and H-ZSM11

	catalyst					
	H-ZSM5			H-ZSM11		
aromatic molecule in feed	toluene	*p*-xylene	1,2,4-TriMB	toluene	*p*-xylene	1,2,4-TriMB
C_1 conversion[b] (%)	54	51	53	57	51	58
methylation rates[c] [10^{-2} mol (mol H s)$^{-1}$]	35	22	3.7	52	33	4.9
disproportionation rates[d] [10^{-2} mol (mol H s)$^{-1}$]	0	1.1	1.6	0	1.3	1.8
% reacted aromatic consumed for disproportionation	0	4.8	31	0	3.7	26
% *p*-xylene within xylenes	59	93	54	55	92	47
% *m*-xylene within xylenes	23	6	36	27	7	41
% *o*-xylene within xylenes	18	1	10	18	1	12

[a]Reaction measured at $p_{toluene}$ = 1.2 kPa, $p_{methanol}$ = 0.3 kPa, 673 K, 5−12 mg of catalyst and 2.3 cm^3 s^{-1} total flow rate. [b]C_1 is methanol and DME. [c]Calculated on the basis of consumption of aromatic reactant in the feed. The isomers are treated also as a reactant. [d]Calculated as eqs 5−7.

Scheme 2. The Reactions Occurring during Toluene Methylation in Medium Pore Zeolites

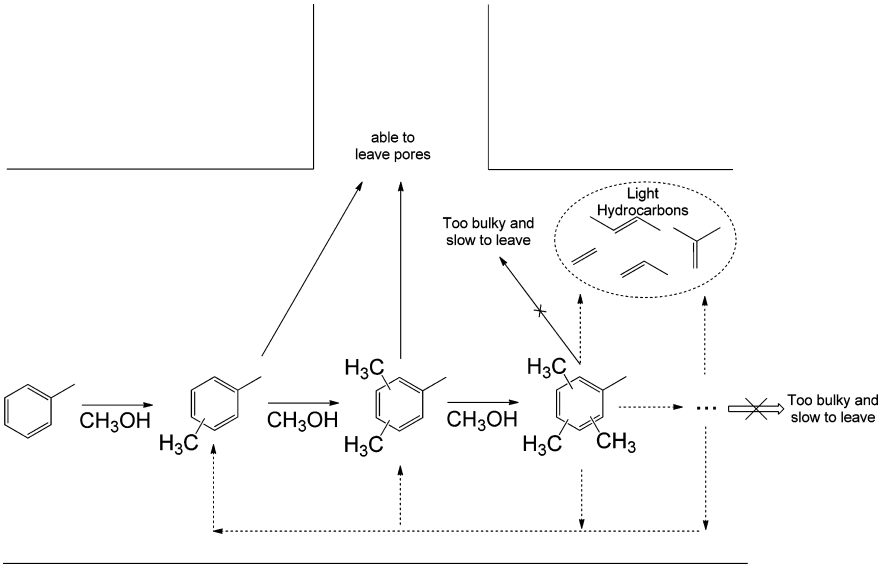

decrease and a slight increase in the rates of methylation and disproportionation, respectively, relative to the rates observed during toluene or *p*-xylene conversions (Table 3). Note that the disproportionation should not be significant,[46−48] and demethylation rates very slow compared to methylation rates[16,41] under the present reaction conditions in medium pore zeolites.

This suggests that a considerable fraction of the "disproportionation" products is formed from the dealkylation of light hydrocarbons from highly methylated aromatics. Some of these less-methylated aromatic molecules are most likely generated as *p*- or *m*-xylenes because ∼90% of xylenes from the reaction between methanol and 1,2,4-TriMB are observed as *p*- or *m*-isomers (Table 3). A drastic decrease in the methylation rate of 1,2,4-TriMB compared with toluene or *p*-xylene in the feed may also indicate that TriMBs are formed as a major product in this reaction pathway and, consequently, decreases the overall conversion of 1,2,4-TriMB. The apparent rate of methylation thus decreases with an increasing number of methyl groups on an aromatic ring (from toluene to *p*-xylene to 1,2,4-TriMB; Table 3) because the aromatic reactant (e.g., xylenes and especially TriMBs) is formed as a product after dealkylation of light hydrocarbons from highly methylated aromatics. For example, the lower conversion of 1,2,4-TriMB and, as a consequence, lower methylation rates during the reaction of 1,2,4-TriMB with methanol are observed compared to methylation with toluene because the converted 1,2,4-TriMB in the feed forms the same reactant molecule again after the aromatic methylation/dealkylation cycle.

In addition, the primary products of higher methylated aromatic reactants (e.g., TetraMBs from 1,2,4-TriMB) have a higher probability to methylate further and dealkylate light hydrocarbons because their diffusion rate is slower than that of the primary products of lower methylated aromatic reactants (e.g., xylenes from toluene). Note that only very small amounts of TetraMB and no penta- or hexamethylbenzenes are able to exit through the zeolite pores. Thus, the lower rate of methylation with an increase in the number of methyl groups on the aromatic ring is also observed, because the primary products of *p*-xylene methylation are larger than the products of toluene methylation (likewise, the primary products of 1,2,4-TriMB methylation than *p*-xylene methylation).

The reaction network for toluene methylation with medium pore zeolites is described in Scheme 2. From the product distribution observed, we speculate that the methylation of toluene continues at least up to TetraMB before the dealkylation of light hydrocarbons becomes more favorable relative to methylation. The stage at which the dealkylation reaction is favored over methylation is reached earlier for the medium pore than for the large pore zeolites; that is, the light

dx.doi.org/10.1021/cs4000766 | ACS Catal. 2013, 3, 817−825

Table 4. Fraction of Methanol Used for the Formation of Light Hydrocarbons with Medium Pore Zeolites

	catalyst			
	H-ZSM11-SC[c]	H-ZSM5	HZSM5-SM[d]	H-ZSM11-LC[e]
"MeOH for LH formation"[a] (%)	32	34	49	64
characteristic diffusion time[b] (s)	1110	2430	6100	30640

[a]"Fraction of "MeOH for LH formation", defined in eq 4. The data obtained from Figure 5. [b]L^2/D determined by *o*-xylene uptake measurement at 403 K using IR spectroscopy. [c]SC = small crystal. [d]SM = surface-modified sample with TEOS. [e]LC = large crystal.

hydrocarbons are dealkylated as a less-methylated aromatic molecule because of less available space in the micropores.[39,45]

This significantly increases the methanol usage toward undesired light hydrocarbons with medium pore zeolites compared with the large ones under these reaction conditions. Once the dealkylation of light hydrocarbons occurs, the residual aromatic molecules diffuse faster and, thus, have a higher probability of leaving the pores before another methylation and dealkylation cycle occurs. The high xylene selectivity in medium pore zeolites is, therefore, a consequence of product shape selectivity; that is, aromatic molecules with multiple methyl groups (most likely four or more) favor splitting off light hydrocarbons, before exiting the zeolite pores, and not transition state selectivity, because highly methylated aromatic molecules can be formed inside the zeolite channels.[15,44]

Effect of Residence Time on Methanol Utilization in Toluene Methylation. With an increase in the residence time of aromatic molecules inside the medium pore zeolites (i.e., with H-ZSM5-SM and H-ZSM11-LC), the methanol usage increases toward the formation of light hydrocarbons ("MeOH for LH formation", Figure 5, striped) and decreases toward methylation of aromatics ("MeOH for aromatics alkylation", Figure 5, open). The increase in methanol usage to light hydrocarbons, observed with surface-modified and large crystal samples, agrees with the hypothesis that most light hydrocarbons are formed via methylation and dealkylation from highly methylated aromatic molecules. Longer residence times of aromatic molecules in H-ZSM5-SM and H-ZSM11-LC provide a higher chance for methylation and dealkylation pathway. In parallel, the "MeOH for aromatics alkylation" fraction decreases because methanol is used for methylating higher methylated aromatics for dealkylation reactions instead of reacting with unreacted aromatic reactant (toluene). This agrees well with the observation that a higher fraction of methanol is incorporated into the aromatic ring of *p*-/*m*-xylenes with larger crystals.[9]

The fraction of methanol used for the formation of light hydrocarbons ("MeOH for LH formation") and the characteristic diffusion time of *o*-xylene (relatively bulky aromatic molecule) with medium pore zeolites are shown in Table 4. The methanol usage to light hydrocarbons increases with the characteristic diffusion time. This suggests strongly that the highly methylated aromatic molecules act as an intermediate to generate light hydrocarbons under these experimental conditions and that increasing the effective residence time of these aromatic molecules shifts the selectivity toward light hydrocarbon formation in medium pore zeolites.

Therefore, a more efficient use of methanol for methylation of toluene is conceivable if the residence time of the bulky aromatic molecules inside the zeolite pores decreases. The increase in diffusivity of the highly methylated aromatic molecules with the large pore zeolites is thus expected to enhance the utilization of methanol toward toluene methylation, yet the decrease in the activation energy with increasing methyl substitution and the lack of product shape selectivity results in a lower xylene selectivity than for the medium pore zeolites. Conceptually, smaller crystal sizes could also enhance methanol usage with medium pore zeolites. Considering the very small crystals (~100 nm) of the H-ZSM5 sample used here, however, it may be challenging to achieve high methanol efficiency toward toluene methylation.

CONCLUSION

The present results show that a significant fraction of C_1 was utilized to form undesired side-products, such as light hydrocarbons and tri- and tetramethylbenzenes, in the toluene methylation reaction. The analysis suggests that the products of toluene methylation, e.g., xylenes and trimethylbenzenes, are readily methylated further in the zeolite pores. These highly methylated aromatic molecules eventually dealkylate light hydrocarbons. With medium pore zeolites (H-ZSM5 and H-ZSM11), the rate of these dealkylation reactions becomes kinetically competitive relative to methylation at an earlier stage, that is, as less-methylated aromatics compared to the large pore zeolites (H-MOR and H-BEA). This pore size effect increases the xylene selectivity within aromatics and the methanol usage toward undesired light hydrocarbons in medium pore zeolites. Likewise for large pore zeolites, the lack of product shape selectivity decreases not only the selectivity of xylenes but also the selectivity to light hydrocarbons. Therefore, the inefficiency of methanol converted during toluene methylation is caused by the further methylation of, for example, xylenes and trimethylbenzenes (aromatic products of toluene) and eventual dealkylation as light hydrocarbons from product shape selectivity. Modest improvements are foreseen for catalytic materials with smaller zeolite crystals.

ASSOCIATED CONTENT

Supporting Information

The time-on-stream behavior on H-ZSM5 and H-BEA, characterization and toluene methylation results of H-BEA with higher acid concentration, XRD of H-ZSM11, SEM images of all zeolites, determination of reaction order in toluene methylation. This material is available free of charge via the Internet at http://pubs.acs.org.

AUTHOR INFORMATION

Corresponding Author

*E-mail: Johannes.Lercher@ch.tum.de.

Notes

The authors declare no competing financial interest.

ACKNOWLEDGMENTS

The authors acknowledge support from the Ministry of Higher Education, Saudi Arabia for the establishment of the Center of Research Excellence in Petroleum Refining and Petrochemicals

at King Fahd University of Petroleum and Minerals (KFUPM). The Deutsche Forschungsgemeinschaft (DFG Project JE 260-10/1) and the "Fonds der Chemischen Industrie" are gratefully acknowledged for the financial support (R.K.). The authors also thank André van Veen, Xianyong Sun, and Oliver Gutiérrez for helpful technical discussions, Xaver Hecht for N_2 physisorption experiments, and Martin Neukamm for SEM images and AAS measurements.

REFERENCES

(1) Tsai, T.; Liu, S.; Wang, I. *Appl. Catal., A* **1999**, *181*, 355−398.
(2) Vermeiren, W.; Gilson, J. P. *Top. Catal.* **2009**, *52*, 1131−1161.
(3) Kulprathipanja, S. *Zeolites in Industrial Separation and Catalysis*; Wiley-VCH: Weinheim, Germany, 2010.
(4) Zhao, Y.; Wu, H.; Tan, W.; Zhang, M.; Liu, M.; Song, C.; Wang, X.; Guo, X. *Catal. Today* **2010**, *156*, 69−73.
(5) Zhu, Z.; Chen, Q.; Xie, Z.; Yang, W.; Li, C. *Microporous Mesoporous Mater.* **2006**, *88*, 16−21.
(6) Kumar, R.; Ratnasamy, P. J. *Catal.* **1989**, *118*, 68−78.
(7) Rao, G. N.; Kumar, R.; Ratnasamy, P. *App. Catal.* **1989**, *49*, 307−318.
(8) Kaeding, W. W.; Chu, C.; Young, L. B.; Weinstein, B.; Butter, S. A. *J. Catal.* **1981**, *67*, 159−174.
(9) Mikkelsen, O.; Rønning, P. O.; Kolboe, S. *Microporous Mesoporous Mater.* **2000**, *40*, 95−113.
(10) Prakash, A. M.; Chilukuri, S. V. V.; Bagwe, R. P.; Ashtekar, S.; Chakrabarty, D. K. *Microporous Mater.* **1996**, *6*, 89−97.
(11) Hibino, T.; Niwa, M.; Murakami, Y. *J. Catal.* **1991**, *128*, 551−558.
(12) Breen, J. P.; Burch, R.; Kulkarni, M.; McLaughlin, D.; Collier, P. J.; Golunski, S. E. *Appl. Catal., A* **2007**, *316*, 53−60.
(13) Mirth, G.; Lercher, J. A. J. *Catalysis* **1994**, *147*, 199−206.
(14) Smit, B.; Maesen, T. L. M. *Nature* **2008**, *451*, 671−678.
(15) Svelle, S.; Joensen, F.; Nerlov, J.; Olsbye, U.; Lillerud, K.; Kolboe, S.; Bjørgen, M. J. *Am. Chem. Soc.* **2006**, *128*, 14770−14771.
(16) McCann, D. M.; Lesthaeghe, D.; Kletnieks, P. W.; Guenther, D. R.; Hayman, M. J.; Van Speybroeck, V.; Waroquier, M.; Haw, J. F. *Angew. Chem., Int. Ed.* **2008**, *47*, 5179−5182.
(17) Arstad, B.; Kolboe, S. *J. Am. Chem. Soc.* **2001**, *123*, 8137−8138.
(18) Bjørgen, M.; Joensen, F.; Lillerud, K.; Olsbye, U.; Svelle, S. *Catal. Today* **2009**, *142*, 90−97.
(19) Olsbye, U.; Bjørgen, M.; Svelle, S.; Lillerud, K.; Kolboe, S. *Catal. Today* **2005**, *106*, 108−111.
(20) Lesthaeghe, D.; Horré, A.; Waroquier, M.; Marin, G. B.; Van Speybroeck, V. *Chem.—Eur. J.* **2009**, *15*, 10803−10808.
(21) De Luca, P.; Crea, F.; Aiello, R.; Fonseca, A.; Nagy, J. B. *Stud. Surf. Sci. Catal.* **1997**, *105*, 325−332.
(22) Derewinski, M.; Machowska, M. *Stud. Surf. Sci. Catal.* **2004**, *154*, 349−354.
(23) Zheng, S.; Heydenrych, H. R.; Jentys, A.; Lercher, J. A. *J. Phys. Chem. B* **2002**, *106*, 9552−9558.
(24) Brunauer, S.; Emmett, P. H.; Teller, E. *J. Am. Chem. Soc.* **1938**, *60*, 308−319.
(25) Lippens, B. C.; Linsen, B. G.; de Boer, J. H. *J. Catal.* **1964**, *3*, 32−37.
(26) Halsey, G. *J. Chem. Phys.* **1948**, *16*, 931−937.
(27) Mirth, G.; Cejka, J.; Lercher, J. A. *J. Catal.* **1993**, *139*, 24−33.
(28) Ivanova, I. I.; Corma, A. *J. Phys. Chem. B* **1997**, *101*, 547−551.
(29) Svelle, S.; Kolboe, S.; Swang, O.; Olsbye, U. J. *Phys. Chem. B* **2005**, *109*, 12874−12878.
(30) Röger, H. P.; Krämer, M.; Möller, K. P.; O'Connor, C. T. *Microporous Mesoporous Mater.* **1998**, *21*, 607−614.
(31) Zheng, S.; Jentys, A.; Lercher, J. A. *J. Catal.* **2006**, *241*, 304−311.
(32) Lesthaeghe, D.; De Sterck, B.; Van Speybroeck, V.; Marin, G. B.; Waroquier, M. *Angew. Chem., Int. Ed.* **2007**, *46*, 1311−1314.
(33) Arstad, B.; Kolboe, S.; Swang, O. *J. Phys. Chem. B* **2002**, *106*, 12722−12726.
(34) Chang, C. D. *Catal . Rev. Sci. Eng.* **1983**, *25*, 1−118.
(35) Stöcker, M. *Microporous Mesoporous Mater.* **1999**, *29*, 3−48.
(36) Röger, H. P.; Möller, K. P.; O'Connor, C. T. *Micro. Mater.* **1997**, *8*, 151−157.
(37) Song, W.; Marcus, D. M.; Fu, H.; Ehresmann, J. O.; Haw, J. F. *J. Am. Chem. Soc.* **2002**, *124*, 3844−3845.
(38) Lesthaeghe, D.; Van Speybroeck, V.; Marin, G. B.; Waroquier, M. *Ind. Eng. Chem. Res.* **2007**, *46*, 8832−8838.
(39) Bjørgen, M.; Svelle, S.; Joensen, F.; Nerlov, J.; Kolboe, S.; Bonino, F.; Palumbo, L.; Bordiga, S.; Olsbye, U. *J. Catal.* **2007**, *249*, 195−207.
(40) Simonetti, D. A.; Ahn, J. H.; Iglesia, E. *J. Catal.* **2011**, *277*, 173−195.
(41) Lesthaeghe, D.; Van der Mynsbrugge, J.; Vandichel, M.; Waroquier, M.; Van Speybroeck, V. *ChemCatChem* **2011**, *3*, 208−212.
(42) Kolvenbach, R.; Ahn, J. H.; Al-Khattaf, S. S.; Jentys, A.; Lercher, J. A. in preparation.
(43) Reitmeier, S. J.; Gobin, O. C.; Jentys, A.; Lercher, J. A. *J. Phys. Chem. C* **2009**, *113*, 15355−15363.
(44) Xu, T.; Barich, D. H.; Goguen, P. W.; Song, W.; Wang, Z.; Nicholas, J. B.; Haw, J. F. *J. Am. Chem. Soc.* **1998**, *120*, 4025−4026.
(45) Svelle, S.; Olsbye, U.; Joensen, F.; Bjørgen, M. *J. Phys. Chem. C* **2007**, *111*, 17.
(46) Kaeding, W. W.; Chu, C.; Young, L. B.; Butter, S. A. *J. Catal.* **1981**, *69*, 392−398.
(47) Fernandez, C.; Stan, I.; Gilson, J.; Thomas, K.; Vicente, A.; Bonilla, A.; Pérez-Ramírez, J. *Chem.—Eur. J.* **2010**, *16*, 6224−6233.
(48) Cheng, X.; Wang, X.; Long, H. *Microporous Mesoporous Mater.* **2009**, *119*, 171−175.